Sensor-Augmented Proning Vest for Continuous Acoustic and Impedance-Based Respiratory Assessment

1st Quentin Goossens
School of Electrical and Computer Engineering
Georgia Institute of Technology
Atlanta, GA, USA
qgoossens3@gatech.edu

2nd Isabelle Coursey
School of Electrical and Computer Engineering
Georgia Institute of Technology
Atlanta, GA, USA
lcoursey3@gatech.edu

3rd Harold Solomon
Office of Commercialization
Quadrant-i
Atlanta, GA, USA
hsolomon@gatech.edu

4th Maxwell Weinmann
Division of Pulmonary, Allergy, Critical Care Medicine
Emory University Hospital
Atlanta, GA, USA
maxwell.weinmann@emory.edu

5th Omer T Inan
School of Electrical and Computer Engineering
Georgia Institute of Technology
Atlanta, GA, USA
omer.inan@ece.gatech.edu

Abstract— Prone positioning improves oxygenation in patients with acute respiratory distress syndrome (ARDS), but traditional methods are labor-intensive and complicates continuous monitoring capabilities. Building on a previously developed mechanically assisted proning vest (V/Q vest), this work focuses on integrating and validating a multi-modal sensor network for non-invasive respiratory monitoring. The system incorporates thoracic bioimpedance electrodes and microphones to derive respiratory parameters, including tidal volume (TV), respiratory rate (RR), phase timing and lung sounds. Data from ten healthy adults were collected during controlled breathing tasks in seated and supine postures. Both seated and supine positions showed strong agreement between IP-derived and spirometer-derived TV, with $R^2 = 0.90$, MAE = 0.16 ± 0.07 L in the seated posture and $R^2 = 0.94$, MAE = 0.12 ± 0.05 L in the supine posture. A flow-based correction method was applied to decouple lung sound intensity from airflow. In the seated posture, mean repeated-measures correlation between uncorrected sound intensity and flow was r = 0.72, dropping to r = 0.01 after correction. In the supine posture, r = 0.71 before correction and r = -0.07 after correction, demonstrating successful flow-decoupling. These results support the feasibility of integrating real-time impedance and acoustic sensing into a therapeutic proning vest, laying the foundation for localized lung monitoring and data-driven respiratory management in critical care.

Keywords—Bioimpedance, Impedance Pneumography, Lung Sounds, Proning, Non-Invasive Sensing, Pulmonary Health

I. INTRODUCTION

In the intensive care unit (ICU), prone positioning is a well-established intervention for improving oxygenation in patients, particularly those with acute respiratory distress syndrome (ARDS). By rotating patients onto their stomachs, proning enhances ventilation-perfusion (V/Q) matching by redistributing pulmonary blood flow to healthier lung regions, in addition to altering lung dynamics and heart-lung interactions. However, the traditional proning process is resource-intensive - requiring up to six clinical staff and approximately 20 minutes per session - and carries risks for both patients and providers [1],

[2]. To address these challenges, prior work led to the development of the pneumatic compression V/Q vest [3], [4], which simulates the therapeutic maneuver of proning while enabling the procedure to be performed more safely and efficiently in under five minutes with only two staff members.

Building on this mechanical platform, we integrated a multimodal sensor network into the pneumatic vest for non-invasive, real-time monitoring of pulmonary physiology. This system leverages our prior work in acoustic sensing of lung sounds (LS) and thoracic impedance measurements to assess respiratory metrics and fluid status [5]. These modalities can be relevant in the ICU, where continuous monitoring guides ventilator settings, detects early signs of deterioration, and
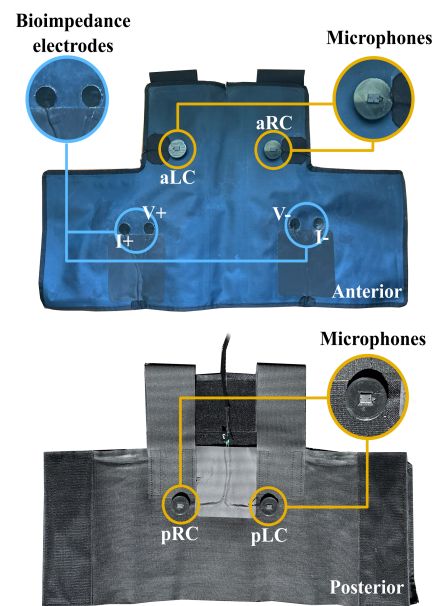

Fig. 1. Integration of the bioimpedance and acoustic sensors into the pneumatic V/Q vest. Both the anterior and posterior faces of the vest are depicted.

evaluates the effectiveness of interventions such as proning. Lung auscultation supports non-invasive respiratory assessment [6], [7], and digital lung sounds have shown value in assessing the inflammatory status of the lungs [8], [9]. Thoracic impedance pneumography (IP) enables tracking of respiratory rate, timing, and volume trends [10], [11]. Additionally, bioimpedance derived metrics offer insight in fluid content changes and localization [5], [12]. Together, these sensing approaches aim to transform the vest into an active diagnostic tool for data-driven respiratory management in critical care settings.

This work validates the sensor-integrated vest in healthy subjects by comparing lung sound and bioimpedance signals to ground truth spirometry data, including a flow-based correction of lung sounds [13], [14]. This comparison assesses signal fidelity, accuracy, and physiological relevance, laying the groundwork for leveraging thoracic impedance and lung sound features to monitor the physiological effects of vest-proning in critical care.

II. METHODS

A. Sensor-Integrated Vest

An instrumented prototype of the V/Q vest was developed (Fig. 1), integrating bioimpedance and acoustic sensing to enable multimodal respiratory monitoring. Four microphones (BU-23173-000, Knowles Electronics LLC., USA) captured lung sounds from the upper anterior and lower posterior quadrants. A custom housing reduced external noise [5], and acoustic signals were sampled at 46.875 kHz. Electrical bioimpedance electrodes captured thoracic signals for impedance pneumography using a tetra-polar configuration, with electrodes near the 5th intercostal space. IP was measured at 100 kHz, sampled at 16 Hz, and calibrated to form complex thoracic impedance vectors [12]. Novel adhesive-free flexible electrodes (23 mm, Silitex, Shieldex, NY, USA) [15] enhanced user comfort. Acoustic and impedance signals were synchronously recorded using a previously validated wearable system [5], which provides up to 18 h of battery life in continuous measurement mode. The vest was inflated to an internal pressure of 10 mmHg during recordings, ensuring stable sensor contact while minimizing discomfort.

B. Data Collection

The study was approved by the Georgia Institute of Technology IRB (IRB2025-90), and all participants provided written informed consent. Ten healthy adults (6 males, 4 females; age 26.6 ± 4.2 years; BMI 20.6 ± 2.9 kg/m²) participated in the study. LS, IP, and spirometry (SP) data were collected during various breathing tasks in seated and supine (30° incline) positions. Ground truth airflow was measured using a spirometer (TSD117A, Biopac Systems, CA) connected to a wired acquisition system (MP150, Biopac Systems, Goleta, CA) at 2 kHz sampling. A nose clip ensured mouth breathing. Each task lasted 1 minute and included normal, shallow, and deep breathing, with shallow and deep tasks performed at 12 and 24 breaths per minute (BrPM), resulting in a total of five tasks per subject.

C. Signal Processing

1) Impedance Signals

Prior to extracting respiratory volume and timing parameters, the raw SP and multi-frequency IP signals were preprocessed (Fig. 2). All preprocessing was conducted in MATLAB (R2023b, Natick, MA). SP and IP signals were first linearly resampled to 100 Hz. The SP flow and IP volume signals were filtered using 10th-order FIR bandpass filters with Kaiser windows in the 0.1-0.8 Hz band, removing high-frequency noise, cardiac artifacts, and baseline drift. A Savitzky-Golay smoothing filter (1500 ms window, second-order polynomial) was then applied to IP signals to further reduce cardiogenic oscillations [11]. Temporal alignment was performed by computing the lag corresponding to the peak cross-correlation between the derivative of the IP signal (a surrogate for flow [11]) and the SP flow.

After preprocessing, SP and IP signals were segmented into 60-second intervals by breathing task. Ground-truth volume signals were derived from SP flow by segmenting breaths at zero-crossing points between inspiration and expiration, followed by integration [16]. To prevent misidentification from noise or irregular breathing, a minimum interval of 0.75 seconds was imposed between zero-crossings. Expiration and inspiration onsets (flow zero-crossings) were mapped to corresponding points on the SP volume signal, corresponding to maximum and minimum lung volumes per cycle. IP segments were first
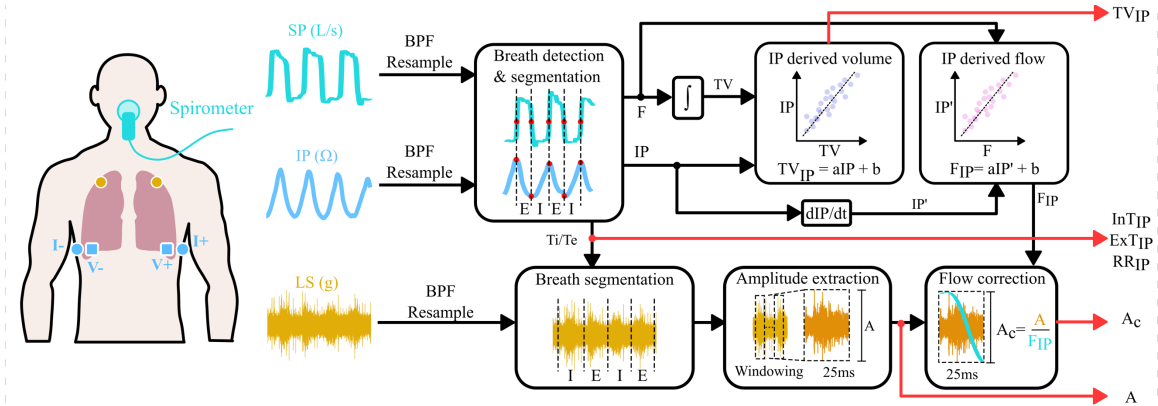

Fig. 2. Overview of the signal processing pipeline used in the present study (vest not shown for clarity). The IP pipeline was used to obtain IP-derived volume (TV$_{IP}$), flow (F$_{IP}$), and respiratory timings (InT$_{IP}$, ExT$_{IP}$, RR$_{IP}$). The LS pipeline was used to obtain sound flow-related amplitude and to correct it using the IP-derived flow.

linearly detrended, followed by breath segmentation using peak detection. Peak detection required a minimum prominence of half the segment's variance and a 1.5-second minimum peak separation. Valleys were identified as the minimum value between peaks. Respiratory features - TV, RR, and phase timings - were extracted using peak and valley timing/amplitude from SP and IP signals. The peak-to-peak amplitude of the integrated SP signal was used as ground-truth TV; IP peak-to-peak values were surrogate estimates. A posture- and subject-specific linear regression model calibrated IP data using the first 30% of each task as training data and the remaining 70% as test data. Reference and IP-derived RR, inspiration time (InT), and expiration time (ExT) were mapped directly. TV estimation accuracy was assessed on test data. Outliers (TV: >2 SD residuals; timing: >3 MAD from median) were excluded. The coefficient of determination (R^2) was calculated across all estimations. The root-mean-square error (RMSE), and mean absolute error (MAE) were computed per subject; results are reported as mean ± SD. Mean absolute percent error (MAPE) was calculated for timing parameters. Correlation and Bland-Altman plots are presented for the TV estimation. Feature extraction, model training, and performance assessments were done in Python.

2) Lung Sound Intensity

Lung sound intensity has been shown to correlate with absolute airflow during breathing [13], [17]. To validate the physiological relevance of vest-recorded sounds, we compared lung sound intensity to spirometer flow recordings. Sounds were recorded from four vest-integrated locations: upper anterior right chest (aRC), upper anterior left chest (aLC), lower posterior right chest (pRC), and lower posterior left chest (pLC). Intensity was computed as the peak-to-peak amplitude within 25 ms non-overlapping windows, averaged over the inspiration and expiration phases. A log transformation of sound intensity improved linearity with airflow.

As prior work shows that the derivative of the IP signal correlates linearly with airflow [11], we calibrated the IP signal derivative to spirometer-measured flow using linear regression on 30% of the data, consistent with the earlier TV calibration. The model was applied to the remaining 70% to generate an IP-derived flow signal for subsequent analysis, supporting autonomous flow estimation after initial calibration. To match the sound intensity extraction, the mean IP-derived flow was
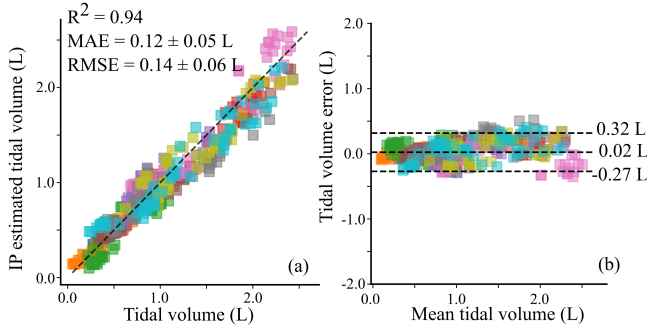

Fig. 3. TV estimation results in the supine position. (a) Correlation plot of IP-estimated TV vs. the spirometer-derived TV. Colors indicate subjects (n = 10). R^2 was calculated across all estimations. MAE and RMSE are reported as mean ± standard deviation across subjects. (b) Corresponding Bland-Altman plot.

TABLE I SUMMARY OF THE PERFORMANCE METRICS FOR ESTIMATING RESPIRATORY PARAMETERS USING IP.

Posture	TV	TV	TV	RR	InT	ExT
	R^2	MAE (L)	RMSE (L)	MAPE (%)		
Seated	0.90	0.16 ± 0.07	0.20 ± 0.10	2.5	7.8	6.9
Supine	0.94	0.12 ± 0.05	0.14 ± 0.06	2.0	5.9	5.4

TABLE II REPEATED MEASURES CORRELATION COEFFICIENTS BETWEEN THE PEAK FLOW AND LOG AMPLITUDE FOR ALL MEASUREMENT LOCATIONS WITHOUT (NC) AND WITH FLOW CORRECTION (C). ALL REPEATED MEASURES CORRELATION P-VALUES FOR NC WERE << 0.001.

Posture	aRC		aLC		pRC		pLC	
	NC	C	NC	C	NC	C	NC	C
Seated	0.76	-0.01	0.77	-0.18	0.74	0.35	0.61	-0.11
Supine	0.75	-0.09	0.72	-0.33	0.70	0.11	0.65	0.05

calculated per window and averaged over the respiratory phases, yielding one sound intensity and one flow value per phase.

To decouple sound intensity from airflow and enable clinical applications, we corrected intensity by dividing the amplitude by mean IP-derived flow per segment. Repeated measures correlation was then used to assess the relationship between sound intensity and flow, both before and after correction. To ensure the analysis considered valid respiratory sounds, only breaths with peak flow exceeding 0.4 L/s were included. Outliers, defined as data points exceeding two standard deviations from the mean, were excluded to improve robustness. All feature extraction and correlation analyses were conducted in Python.

III. RESULTS

Table I summarizes the results of respiratory parameters estimation using IP data across all subjects. Fig. 3 shows the correlation plot and the corresponding Bland-Altman plots comparing the IP estimated TV to the reference TV across all subjects in both seated and supine positions. Results from the supine position are highlighted due to their clinical relevance in hospital settings, where patients are typically in a supine posture. Across both postures, the IP-derived TV demonstrated strong agreement with spirometry, with R^2 values equal to or exceeding 0.90 and mean absolute errors comparable or superior to other wearable form factors [10], [16], [18]. Respiratory timing parameters, respiratory rate, inspiration time, and expiration time, also showed consistent alignment with reference values (< 3% MAPE for RR, < 0.5s error for InT and ExT), confirming the system's accuracy in capturing dynamic breathing patterns. These findings support the use of vest-integrated impedance sensing for continuous, non-invasive respiratory monitoring and are in line with previous reports using wearable form factors for thoracic bioimpedance measurement. The results further validate the potential of integrating such sensing modalities into therapeutic devices to enable data-driven respiratory care in critical settings. Fig. 4 shows the regression results for the acoustic analysis. Two subjects were excluded due to insufficient airflow amplitudes. All measurement locations exhibited a significant positive correlation between uncorrected lung sound intensity (NC) and airflow (mean repeated measures r = 0.71). Following correction (C), this correlation was effectively eliminated (mean repeated measures r = -0.03), indicating successful decoupling of sound intensity from airflow. Notably, the anterior microphones demonstrated stronger correlations and/or more consistent linear relationships between different subjects than the posterior microphones,
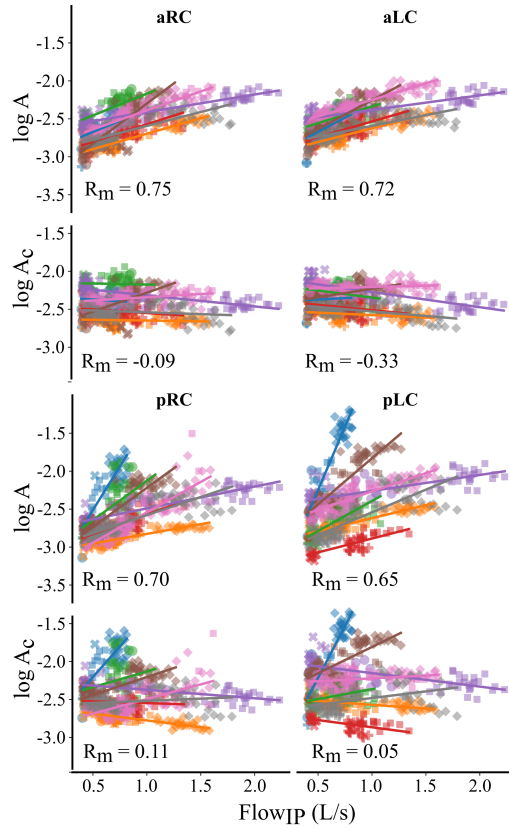
Fig. 4. Regression plots between sound intensity and the IP-derived flow across the four microphone locations measured in the supine position. Both non-corrected (log A) and flow-corrected (log A_c) sound intensities are shown. Colors indicate subjects (n = 8), and markers represent breathing tasks. Repeated measures correlation (r_m) is reported.

which may be attributed to motion artifacts and backing pressure affecting the posterior sensors during the supine position. While this limits the utility of posterior signals in their current form, improved sensor mounting and signal processing strategies could mitigate these issues. Table II provides an overview of the repeated measures correlation coefficients for all measurement locations, summarizing the relationships between lung sound intensity and airflow before and after correction.

IV. Conclusion

This study demonstrates the feasibility of integrating multi-modal sensors within the V/Q vest, a mechanically assisted proning system, to enable continuous, non-invasive monitoring of respiratory physiology. By validating lung sound and thoracic impedance signals against spirometry across multiple breathing conditions and postures, we show that the sensor-augmented V/Q vest can reliably estimate key respiratory metrics such as TV, RR, and phase timing. While validated in healthy subjects, this work lays the groundwork for extension to ARDS patients, where altered lung mechanics and fluid distribution may highlight the vest's clinical value. Additionally, we introduce and validate a flow-correction technique for lung sound intensity, enhancing the interpretability of acoustic signals for potential clinical use. These findings establish a foundation for transforming the V/Q vest into an active monitoring platform supporting real-time, data-driven decision-making in critical care. The design of the electrode array enables future expansion

toward regional lung impedance mapping, offering insight into fluid distribution and ventilation patterns - critical parameters for managing complex pulmonary conditions without imaging.

References

[1] N. Wiggermann, J. Zhou, and D. Kumpar, "Proning Patients With COVID-19: A Review of Equipment and Methods," Hum. Factors J. Hum. Factors Ergon. Soc., vol. 62, no. 7, pp. 1069–1076, Nov. 2020.

[2] S. Cotton, Q. Zawaydeh, S. LeBlanc, A. Husain, and A. Malhotra, "Proning during covid-19: Challenges and solutions," Heart Lung, vol. 49, no. 6, pp. 686–687, 2020.

[3] A. B. Ambrose, L. Tiziani, D. J. Ward, M. Weinmann, and F. L. Hammond, "A Pneumatic Compression Vest for Transthoracic Manipulation of Ventilation-Perfusion in Critical Care Patients with Acute Respiratory Distress Syndrome Caused by COVID-19," in 2021 Design of Medical Devices Conference: American Society of Mechanical Engineers, 2021, p. V001T04A007.

[4] A. B. Ambrose, J. F. Detelich, M. Weinmann, and F. L. Hammond, "Evaluation of a Pneumatic Vest to Treat Symptoms of ARDS Caused by COVID-19," J. Med. Devices, vol. 16, no. 1, p. 011004, 2022.

[5] J. A. Sanchez-Perez et al., "A Wearable Multimodal Sensing System for Tracking Changes in Pulmonary Fluid Status, Lung Sounds, and Respiratory Markers," Sensors, vol. 22, no. 3, p. 1130, 2022.

[6] A. Bohadana, G. Izbicki, and S. S. Kraman, "Fundamentals of Lung Auscultation," N. Engl. J. Med., vol. 370, no. 8, pp. 744–751, 2014.

[7] M. Sarkar, I. Madabhavi, N. Niranjan, and M. Dogra, "Auscultation of the respiratory system," Ann. Thorac. Med., vol. 10, no. 3, p. 158, 2015.

[8] F. Pancaldi et al., "VECTOR: An algorithm for the detection of COVID-19 pneumonia from velcro-like lung sounds," Comput. Biol. Med., vol. 142, p. 105220, 2022.

[9] J. A. Sanchez-Perez et al., "Enabling Continuous Breathing-Phase Contextualization via Wearable-Based Impedance Pneumography and Lung Sounds: A Feasibility Study," IEEE J. Biomed. Health Inform., vol. 27, no. 12, pp. 5734–5744, 2023.

[10] J. A. Berkebile, S. A. Mabrouk, V. G. Ganti, A. V. Srivatsa, J. A. Sanchez-Perez, and O. T. Inan, "Towards Estimation of Tidal Volume and Respiratory Timings via Wearable-Patch-Based Impedance Pneumography in Ambulatory Settings," IEEE Trans. Biomed. Eng., vol. 69, no. 6, pp. 1909–1919, 2022.

[11] V.-P. Seppa, J. Viik, and J. Hyttinen, "Assessment of Pulmonary Flow Using Impedance Pneumography," IEEE Trans. Biomed. Eng., vol. 57, no. 9, pp. 2277–2285, 2010.

[12] S. Mabrouk et al., "Robust Longitudinal Ankle Edema Assessment Using Wearable Bioimpedance Spectroscopy," IEEE Trans. Biomed. Eng., vol. 67, no. 4, Art. no. 4, 2020.

[13] S. S. Kraman, "The Relationship Between Airflow and Lung Sound Amplitude in Normal Subjects," Chest, vol. 86, no. 2, pp. 225–229, 1984.

[14] J. A. Sanchez-Perez, S. Mabrouk, G. C. Ozmen, J. A. Berkebile, and O. T. Inan, "Towards Wearable-Based Lung Sound Intensity Assessment Leveraging Impedance Pneumography," in IEEE SENSORS, 2023, pp. 1–4.

[15] C. J. Nichols, S. A. Mabrouk, G. C. Ozmen, A. H. Gazi, and O. T. Inan, "Validating Adhesive-Free Bioimpedance of the Leg in Mid-Activity and Uncontrolled Settings," IEEE Trans. Biomed. Eng., vol. 70, no. 9, pp. 2679–2689, 2023.

[16] H. Jung, S. Mabrouk, and O. T. Inan, "Impedance Pneumography: Assessment of Dual-Frequency Calibration Approaches," in 2021 IEEE BSN, 2021, pp. 1–4.

[17] E. Messner, M. Hagmüller, P. Swatek, F.-M. Smolle-Jüttner, and F. Pernkopf, "Impact of Airflow Rate on Amplitude and Regional Distribution of Normal Lung Sounds:," in Proceedings of the 10th International Joint Conference on Biomedical Engineering Systems and Technologies: SCITEPRESS - Science and Technology Publications, 2017, pp. 49–53.

[18] M. Klum, M. Urban, A.-G. Pielmus, and R. Orglmeister, "Wearable Impedance Pneumography," Curr. Dir. Biomed. Eng., vol. 6, no. 3, pp. 233–236, 2020.